This article was downloaded by: *[Li, Zhe]*
On: *13 October 2010*
Access details: *Access Details: [subscription number 928020538]*
Publisher *Taylor & Francis*
Informa Ltd Registered in England and Wales Registered Number: 1072954 Registered office: Mortimer House, 37-41 Mortimer Street, London W1T 3JH, UK

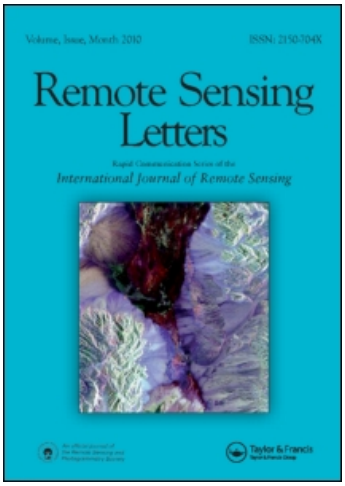

Remote Sensing Letters
Publication details, including instructions for authors and subscription information:
http://www.informaworld.com/smpp/title~content=t915281289

Integrating Mahalanobis typicalities with a neural network for rubber distribution mapping

Zhe Li[ab]; Jefferson M. Fox[b]
[a] Canada Center for Remote Sensing, Natural Resources Canada, Ottawa, ON, Canada [b] East-West Center, Honolulu, HI, USA

First published on: 13 October 2010

To cite this Article Li, Zhe and Fox, Jefferson M.(2011) 'Integrating Mahalanobis typicalities with a neural network for rubber distribution mapping', Remote Sensing Letters, 2: 2, 157 — 166, First published on: 13 October 2010 (iFirst)
To link to this Article: DOI: 10.1080/01431161.2010.505589
URL: http://dx.doi.org/10.1080/01431161.2010.505589

PLEASE SCROLL DOWN FOR ARTICLE

Full terms and conditions of use: http://www.informaworld.com/terms-and-conditions-of-access.pdf

This article may be used for research, teaching and private study purposes. Any substantial or systematic reproduction, re-distribution, re-selling, loan or sub-licensing, systematic supply or distribution in any form to anyone is expressly forbidden.

The publisher does not give any warranty express or implied or make any representation that the contents will be complete or accurate or up to date. The accuracy of any instructions, formulae and drug doses should be independently verified with primary sources. The publisher shall not be liable for any loss, actions, claims, proceedings, demand or costs or damages whatsoever or howsoever caused arising directly or indirectly in connection with or arising out of the use of this material.

Remote Sensing Letters
Vol. 2, No. 2, June 2011, 157–166

Taylor & Francis
Taylor & Francis Group

Integrating Mahalanobis typicalities with a neural network for rubber distribution mapping

ZHE LI*†‡ and JEFFERSON M. FOX‡
†Canada Center for Remote Sensing, Natural Resources Canada, Ottawa, ON K1A 0Y7, Canada
‡East-West Center, Honolulu, HI 96848, USA

(*Received 16 February 2010; in final form 28 June 2010*)

Accurate rubber distribution mapping is critical to the study of its expansion and to provide a better understanding of the consequences of land-cover and land-use change on carbon and water cycles. Employing Mahalanobis typicalities as inputs to a hard classifier to enhance the capability of generalization has not previously been explored. This letter presents a novel approach by integrating Mahalanobis typicalities with the multi-layer perceptron (MLP) neural network for mapping of rubber. A case study from the Thai–Lao and Sino–Lao borders was conducted using Advanced Spaceborne Thermal Emission and Reflection Radiometer (ASTER) data. Different combinations of the nine ASTER bands including Visible and Near Infrared (VNIR) and Short-wave Infrared (SWIR), Normalized Difference Vegetation Index (NDVI) and Mahalanobis typicalities were used as input variables to the MLP. Results indicate that including Mahalanobis typicalities as input variables can improve the MLP's performance and increase the user's accuracy of rubber mapping.

Downloaded By: [Li, Zhe] At: 13:52 13 October 2010

1. Introduction

The Pará rubber tree (*Hevea brasiliensis*) initially grew only in the Amazon Rainforest. Today Rubber plantations are expanding rapidly throughout montane mainland Southeast Asia (MMSEA) (Fox and Vogler 2005) and rubber has become the major commercial crop replacing traditional agriculture and secondary forests (Ziegler *et al.* 2009). An abrupt shift in land use from ecologically important tropical forests and traditionally managed swidden fields to large-scale rubber plantations can result in a great loss of ecosystem services and affect local energy, water and carbon fluxes (Van Ranst *et al.* 1996, Li *et al.* 2007, Hu *et al.* 2008). Accurate mapping of rubber distribution and differentiating rubber from second-growth forests is critical to the study of rubber expansion and its implications for water and carbon dynamics in MMSEA.

Remotely sensed imagery classification is one of the main means of deriving land-use and land-cover information. Taking advantages of their non-parametric requirements, numerous machine learning techniques have been widely used in imagery classification. However, a major challenge for mapping mature rubber is overestimation by misclassifying second-growth forests as rubber, because first the area of rubber occupies a very small proportion relative to other land-cover types such as

*Corresponding author. Email: Zhe.Li@NRCan.gc.ca

Remote Sensing Letters
ISSN 2150-704X print/ISSN 2150-7058 online © 2011 Taylor & Francis
http://www.tandf.co.uk/journals
DOI: 10.1080/01431161.2010.505589

forests and croplands, and second rubber trees have similar multi-spectral reflectance characteristics with tropical evergreen vegetation.

Many researchers use ancillary data in addition to spectral bands to improve remote sensing classification accuracy. These data may include information regarding terrain (e.g. elevation, slope and aspect), environmental (e.g. temperature and moisture), textural (e.g. fractal dimension), contextual factors (e.g. spatial dependence) (Ghimire *et al.* 2010) and enhanced or transformed images such as principal components and tasselled cap components (Jin and Sader 2005). Some researchers employ soft image fractions as inputs to a hard classifier to yield higher classification accuracy. For example, Roberts *et al.* (2002) combined spectral mixture analysis (SMA) fractions as inputs to a classification tree for large area land-cover mapping. As rubber is a planted crop in the MMSEA region, its distribution is not greatly affected by terrain, environmental factors or land suitability, but rather by the availability of land. We confirmed this hypothesis when we conducted rubber surveys in both suitable and unsuitable areas for rubber plantations in northeast Thailand. Initial experiments indicate that including growth suitability factors in rubber distribution mapping contributes little to improving accuracy. Therefore, we decided to explore new factors to highlight features of rubber that can distinguish it from other species. Inspired by Roberts *et al.* (2002), in this study, we are particularly interested in examining the potential for integrating Mahalanobis typicalities with the multilayer perceptron (MLP) neural network for rubber classification. Although numerous studies of remote sensing classification using the MLP neural network have been conducted and both Mahalanobis distance (MD) based and neural approaches are individually well established, incorporating these two techniques in vegetation classification has not been previously explored.

Downloaded By: [Li, Zhe] At: 13:52 13 October 2010

2. Methodology

2.1 *Mahalanobis typicality*

In statistics, MD is a distance measure introduced by P.C. Mahalanobis in 1936 (Foody *et al.* 1992). It is based in part on correlations between variables and is a measure of class relative distance to the class mean, scaled by the class covariance. MD is a multivariate equivalent of a z-score and is expressed as

$$D = \sqrt{(\boldsymbol{x} - \boldsymbol{\mu}_i)^T \mathbf{V}_i^{-1} (\boldsymbol{x} - \boldsymbol{\mu}_i)} \tag{1}$$

where $\boldsymbol{x}$ is the data vector for the pixels in all wavebands, $\boldsymbol{\mu}_i$ the mean vector for class i over all pixels, $\mathbf{V}_i$ the variance/covariance matrix for class i and T the transpose of the matrix (Foody *et al.* 1992).

Mahalanobis distance is a useful way of determining similarity of an unknown sample to a known group of samples. As Mahalanobis distance has a χ^2 with degrees of freedom equal to the number of independent variables minus 1, it can be used to produce the measure known as *Typicality Probability* (or simply *Typicality*). Specifically, *Typicality* is the probability of any location having a MD greater or equal to that observed at the location of interest (figure 1). Locations having attributes identical to the multivariate centroid have a typicality of 1.0, with less typical locations approaching a typicality of 0.0 at the limits of the distribution (Li and Eastman 2010). The output of *Mahalanobis typicality* is not a single classified land-

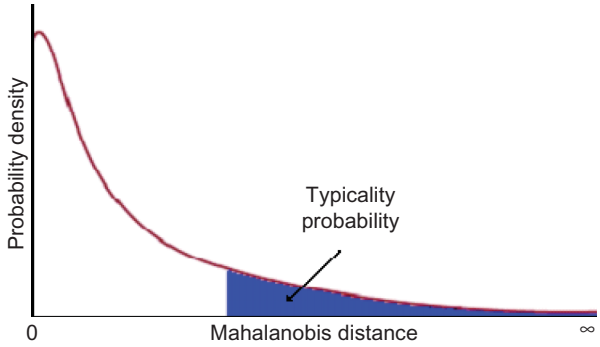

Figure 1. Graphical representation of the Mahalanobis typicalities (typicality probability).

Downloaded By: [Li, Zhe] At: 13:52 13 October 2010

cover map, but rather, a set of images (one per class) that express the typicality of the pixel relative to the training classes.

The concept of typicality expresses the degree to which the values of a set of input variables at a location are typical of known instances of a specific class (Foody *et al.* 1992, Eastman *et al.* 2005). In contrast to relative measures of class membership derived from maximum likelihood method, the typicalities suggest whether it is reasonable to assume that a case really belongs to a particular class because they are a measure of the absolute strength of class membership (Foody 2002). That is, a high typicality to an allocated class necessarily leads to a high membership, but not vice versa. For example, a very low typicality to the allocated class could indicate that the case is actually a member of an untrained class (Foody 2002). The typicality can be used to refine classifications such as to find areas that are misclassified because of missing training data (Sangermano and Eastman 2007). Recently Mahalanobis typicality has been applied to species distribution modelling (Hernandez *et al.* 2008).

2.2 *Multi-layer perceptron neural network*

The MLP is the most widely used artificial neural network model for pattern recognition (Hinton and Salakhutdinov 2006). In an MLP, nodes (or neurons) are organized into different layers (one input layer, one output layer and one or more hidden layers), each generally fully interconnected to the following layer. The input layer takes input patterns as represented by the variables. The output layer outputs a measure of support, typically forced to a 0–1 range by the activation layer function, for each land-cover class. The role of the hidden layer nodes, in combination with the connection weights, serves to create a set of hyperplanar discriminant functions that can separate the variable space (image band space in this case) into regions associated with the different classes (Richards and Jia 2006). An MLP has to be trained to perform a specific task. The most popularly used training algorithm is the back propagation (BP) method, which iteratively reduces the error between the desired and actual output values through a gradient descent technique known as the delta rule. The forward and backward passes continue until the network has 'learned' the characteristics of all the classes and the root mean square error (RMSE) between fitted and ideal activation levels reaches an acceptable value.

2.3 *Data and methods*

The study sites we chose for the experiments were the Thai–Lao (upper left: 103°27′39″E, 18°37′38″N; lower right: 103°59′39″E, 18°1′44″N) and the Sino–Lao (upper left: 100°49′58″E, 21°39′25″N; 101°32′20″E, 21°0′30″N) borders, where rubber has been widely and intensively planted, especially in Nongkai province of Thailand and Yunnan province of China, where rubber planting has a long history.

Vegetation mapping has relied on medium spatial resolution imagery from multi-spectral sensors such as Landsat Thematic Mapper (TM)/Enhanced Thematic Mapper Plus (ETM+), hyperspectral imagery, high-resolution imagery (e.g. IKONOS and Quickbird) and multi-spectral and multi-temporal imagery such as Moderate Resolution Imaging Spectroradiometer (MODIS). Recently, the Advanced Spaceborne Thermal Emission and Reflection Radiometer (ASTER) has been of special interest to remote sensing of environment in that it has relatively broad spectral resolution and relatively fine spatial resolution. We chose ASTER imagery for the rubber mapping as it provides visible and near–infrared bands (VNIR) with 15 m pixels and short-wave infrared bands (SWIR) with 30 m pixels wavelengths that are particularly important for vegetation discrimination.

The ASTER data used in this study were the orthorectified and terrain-corrected On-Demand L3 products which were acquired from Land Processes Distributed Active Archive Center (LPDAAC). An ASTER granule (scene) covers approximately 60×60 km^2. We chose dry season images to reflect dry season vegetation phenology. The image for Thai–Lao border was acquired on 24 April 2005 and for Sino–Lao border on 8 February 2005. We used NASA's Landsat GeoCover products to identify land-use and land-cover types for use as training sites. Rubber identification was primarily based on global positioning system (GPS) ground reference samples collected from field and high-resolution IKONOS images from Google Earth. As the main purpose of the experiment was to map rubber distribution, only five broad categories were digitized for the Sino–Lao site. As mature rubber trees are easily confused with eucalyptus, which is widely planted in Thailand, the eucalyptus category was indentified as a separate class for the Thai–Lao site (not for the Sino–Lao site). For both the two sites, rubber is indentified as a single class (table 1). The numbers of rubber samples for the two sites account for 0.029 and 0.214% of the total image pixels, respectively. Separate testing sites were also developed for classification accuracy assessment.

An image fusion technique was used to convert the ASTER VNIR and SWIR bands into the same resolution. To do this, the SWIR bands (S4–S9) were first transformed

Table 1. Number of training and testing pixels for the two study sites.

		Thai–Lao border study site			Sino–Lao border study site		
Class ID	Class name	Training pixels	% of image	Testing pixels	Training pixels	% of image	Testing pixels
1	Rubber	3,453	0.029	6,807	33,439	0.21	48,880
2	Eucalyptus	1,499	0.013	2,819	N/A	N/A	N/A
3	Water	45,980	0.388	11,657	3,270	0.02	508
4	Paddy	4,449	0.038	2,135	7,600	0.05	2,694
5	Bare	3,387	0.029	401	184	0.00	845
6	Forest	33,688	0.284	3,216,232	132,994	0.82	50,521
	Total	92,456	0.780	3,240,051	177,487	1.09	103,448

Downloaded By: [Li, Zhe] At: 13:52 13 October 2010

Table 2. Input variable combinations for the MLP.

Name	Input variable combination
VC1	VNIR
VC2	VINR + SWIR
VC3	VNIR + NDVI
VC4	VNIR + SWIR + NDVI
VC5	VNIR + typicality
VC6	VNIR + SWIR + typicality
VC7	VNIR + NDVI + typicality
VC8	VNIR + SWIR + NDVI + typicality
VC9	NDVI + typicality
VC10	Typicality

into six principal components, and then these components were back-projected after replacing the first component with a higher-resolution image, which is usually a panchromatic image. As the panchromatic image is not available for ASTER data, we used the first component (accounting for over 96% of total variance) generated from the three VNIR bands, to serve as the higher-resolution image. As the VNIR component 1 is highly correlated with the SWIR component 1 ($r = 0.94$), the image fusion technique is less likely to produce major artefacts. This image enhancement approach produced ASTER SWIR pixels with a sampling of 15 m, instead of the original 30 m.

We examined a variety of combinations of input variables for the land-cover classifications. The input metrics incorporate ASTER multi-spectral bands (VNIR and enhanced SWIR), normalized difference vegetation index (NDVI) and typicalities derived from the MD classifier (see table 2). With the same training data, three ASTER VNIR bands and six enhanced SWIR bands were used as input variables to generate Mahalanobis typicalities. Six and five typicality images (corresponding to the six and five classes) were created for the Thai–Lao and Sino–Lao images, respectively.

The neural network model used in this study was the MLP module of IDRISI 16.0 Taiga. The training of the MLP neural network is a heuristic process. For each variable combination, the MLP was run 20 times using fixed iterations but with different learning rates, which are sensitive to convergence of training. The best results achieved from each of the 20 trials were chosen for analysis. To avoid over-training or under-training the classifier, 30,000 and 10,000 iterations were set for Thai–Lao and Sino–Lao images, respectively, so that both the training RMSE and testing RMSE decreased to between 0.001 and 0.1. To make the MLP converge quickly but with less fluctuation, the learning rate was set to 0.0001 for both study sites. To maintain the best capability of MLP's generalization, the numbers of hidden layer neurons were set between 8 and 20 by using the following equation, where INT represents the operation of rounding to the nearest integer number.

$$N_{\text{hidden}} = \text{INT}\left(\sqrt{N_{\text{input}} \times N_{\text{output}}}\right) \tag{2}$$

3. Validation

Separate and independent testing sites were developed to validate performance of the MLP model with different input variable combinations. Error matrixes were

Downloaded By: [Li, Zhe] At: 13:52 13 October 2010

generated for each of the 10 classification results with the 10 different variable combinations for each of the two study sites. Besides total accuracy and overall kappa coefficient for all the classes, we also looked at kappa coefficient, producer's accuracy and user's accuracy for the rubber category (Congalton 1991). In addition, we also used a single index to comprehensively evaluate the performance of the classification results, the geometric mean of indices (GMI):

$$\mathrm{GMI} = \left(\prod_{i=1}^{n} a_i\right)^{1/n} = \sqrt[n]{a_1 \cdot a_2 \cdot \cdots \cdot a_n} \tag{3}$$

where a_1–a_n represent n assessment indices that have the same tendency of goodness when they monotonically increase or decrease, and have the same scales. Specifically, in this study, a_1–a_n represent five indices, that is, total accuracy and overall kappa coefficient for all categories, kappa coefficient, producer's accuracy and user's accuracy for the rubber category. The advantage of the geometric mean is that it indicates the central tendency or typical value of a set of numbers in contrast to the arithmetic mean. For example, suppose we have two sets of numbers, 0.5 and 0.5 versus 0.1 and 0.9, representing user's accuracy and producer's accuracy, respectively, for each set. Both the sets have the same arithmetic mean, namely, 0.5, but different geometric means (0.5 and 0.3, respectively). Obviously, the geometric mean is more informative and reasonable as we prefer the former dataset over the latter, which achieved too low user's accuracy (0.1).

Downloaded By: [Li, Zhe] At: 13:52 13 October 2010

4. Results and discussion

Figure 2(*a*) shows the land-cover classification results using different combinations of variables for the Thai–Lao border site. Table 3 and figure 3(*a*) show the accuracy assessment. In the Thai–Lao border site, rubber and eucalyptus are mainly distributed on the Thai side (south of the Mekong River). In Laos (north of the Mekong), land cover was dominated by forests and paddy rice and very little rubber or eucalyptus. As can be seen from figure 2(*a*): (*i*) to (*j*), with only spectral information VNIR and/or SWIR (VC1 and VC2), the MLP classifier overestimated the number of rubber pixels (in red), namely, it misclassified a large number of forest pixels as rubber in Laos, which caused high commission errors (or low user's accuracies (0.005 and 0.046, respectively)) for the rubber class (figure 3(*a*)). Although the producer's accuracies and kappa coefficients for the rubber class increased when the NDVI was introduced, overestimation of rubber still remained (figure 2(*a*): (*k*) using VC3 and (*l*) using VC4). However, it can be seen from figure 3(*a*) that the GMI sharply increased at VC5 from 0.124 to 0.583 when the Mahalanobis typicalities were included (from figure 2(*a*): (*m*) to (*r*)), and all six variable combinations show similar trends in accuracy. All six maps show reasonable results in comparison with maps (*i*)–(*l*). The GMI, total accuracy and overall kappa coefficient for the six classes and the user's accuracy for the rubber class are notably higher than those without including the typicalities, although they did not perform better than those using VC2, VC3 and VC4 in terms of the producer's accuracy and kappa coefficient for the rubber class. For land-cover mapping over a large spatial area, a low commission error (high user's accuracy) is extremely important, as the rubber accounts for a very small proportion relative to the forest and other vegetation. Of the 10 maps created, figure 2(*a*): (*r*) with only typicality information

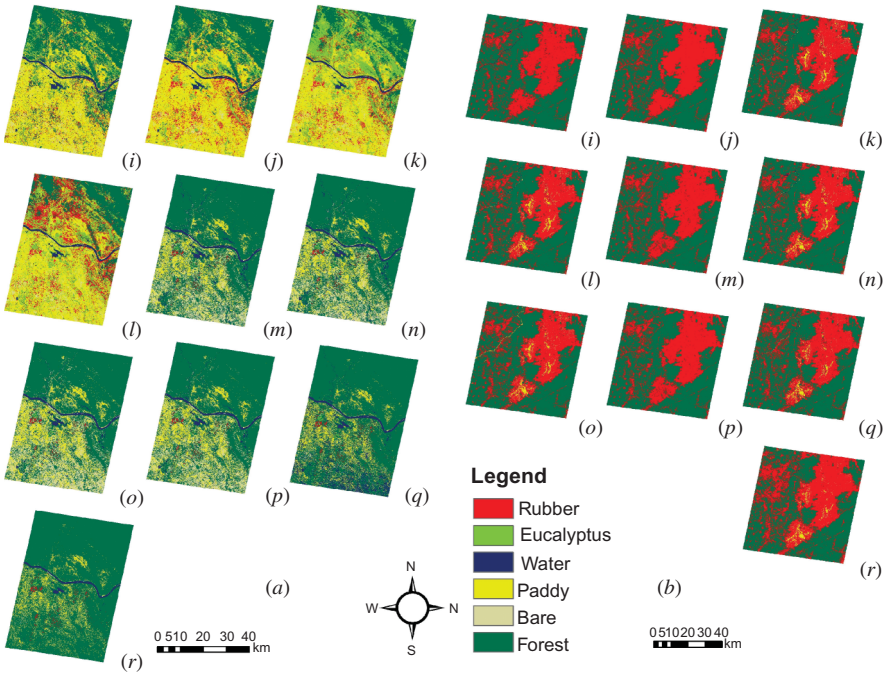

Figure 2. (*a*): Land-cover classifications for Thai–Lao border site with 10 different metrics; and (*b*): Land-cover classifications for Sino–Lao border site with 10 different variables combinations. (*i*)–(*r*) correspond to variable combinations VC1–VC10 (see table 2 for details), respectively.

Table 3. Accuracy assessment of classification for the Thai–Lao study site.

Assessment indices	VC1	VC2	VC3	VC4	VC5	VC6	VC7	VC8	VC9	VC10	MD
Total accuracy	0.766	0.695	0.423	0.380	0.988	0.989	0.990	0.991	0.993	**0.997**	0.680
Overall Kappa coefficient	0.034	0.036	0.016	0.014	0.461	0.468	0.493	0.529	0.582	**0.757**	0.030
User's accuracy for rubber	0.005	0.046	0.026	0.006	**0.977**	0.976	0.976	**0.977**	0.976	**0.977**	0.014
Producer's accuracy for rubber	0.050	0.878	0.935	**0.946**	0.390	0.402	0.391	0.389	0.404	0.392	0.656
Kappa coefficient for rubber	0.031	0.873	**0.930**	0.920	0.389	0.401	0.390	0.389	0.404	0.391	0.619
Geometric mean (GMI)	0.046	0.245	0.172	0.124	0.583	0.592	0.592	0.600	0.620	**0.647**	0.163
Arithmetic mean	0.177	0.506	0.466	0.453	0.641	0.647	0.648	0.655	0.672	**0.703**	0.400

Note: VC1–VC10 represent variable combinations, see table 2 for details; MD represents Mahalanobis distance classifier; numbers in bold represent the highest values for each accuracy category.

Downloaded By: [Li, Zhe] At: 13:52 13 October 2010

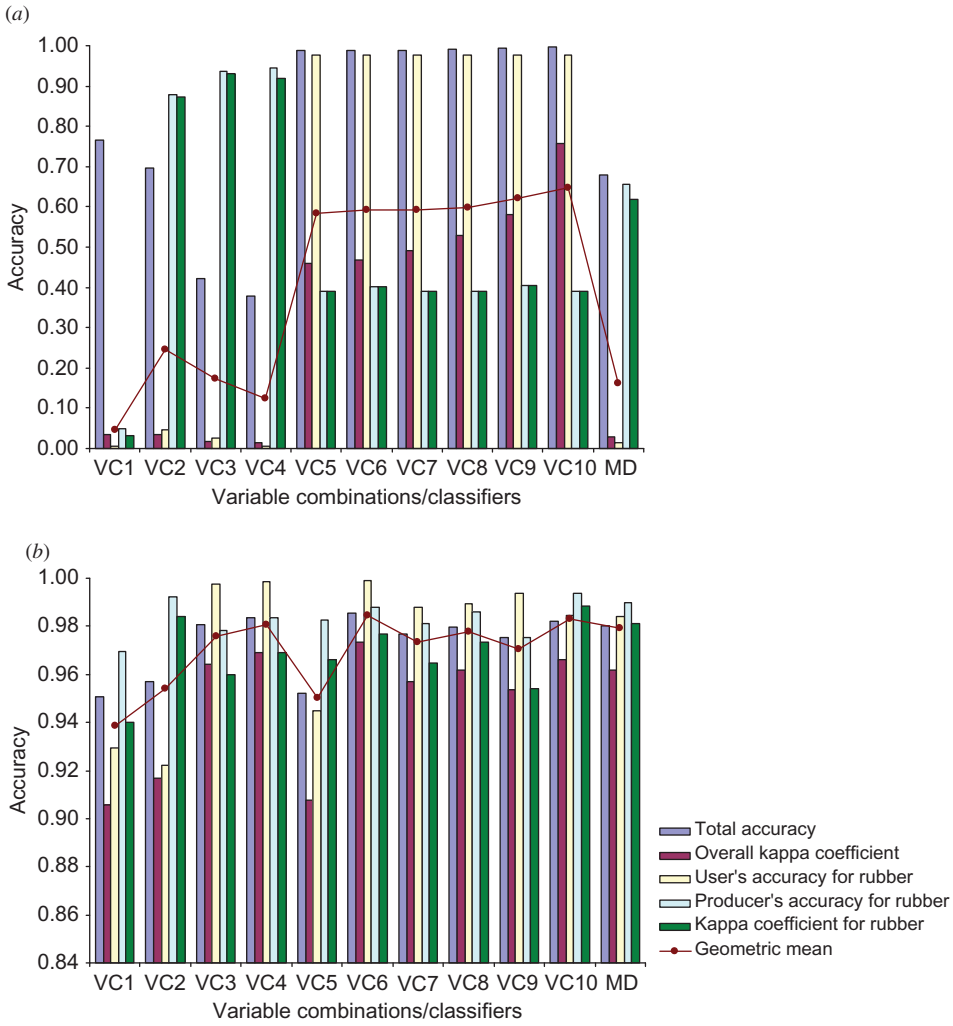

Figure 3. Accuracy assessment for classifications in: (*a*) Thai–Lao border; and (*b*) Sino–Lao border, with different variable combinations/classifiers (VC1–VC10 represent variable combinations, see table 2 for details; MD represents Mahalanobis distance classifier).

Downloaded By: [Li, Zhe] At: 13:52 13 October 2010

(VC10) achieved the highest GMI, total accuracy, overall kappa coefficient, single kappa coefficient and user's accuracy. To examine whether integrating Mahalanobis typicalities in the MLP outperforms MD classifier itself, a classification with the MD classifier using the VC4 inputs was also conducted. It is interesting to see that the MD slightly outperformed the MLP with VC4 inputs in terms of total accuracy, overall kappa coefficient and user's accuracy for rubber class, whereas the MLP notably outperformed the MD when using the same input variable combinations plus the Mahalanobis typicalities (VC8). And all MLPs integrating the typicalities provided better results than the MD in terms of most of the indices.

For the Sino–Lao border site, about 10 times of rubber training pixels than the Thai–Lao border site were used (table 1), because rubber is extensively planted in

Table 4. Accuracy assessment of classification for the Sino–Lao study site.

Assessment indices	VC1	VC2	VC3	VC4	VC5	VC6	VC7	VC8	VC9	VC10	MD
Total accuracy	0.951	0.957	0.981	0.983	0.952	**0.986**	0.977	0.980	0.975	0.982	0.980
Overall Kappa coefficient	0.906	0.917	0.964	0.969	0.908	**0.973**	0.957	0.962	0.954	0.966	0.962
User's accuracy for rubber	0.929	0.922	0.998	0.999	0.945	**0.999**	0.988	0.989	0.994	0.984	0.984
Producer's accuracy for rubber	0.970	0.992	0.978	0.983	0.983	0.988	0.981	0.986	0.975	**0.994**	0.990
Kappa coefficient for rubber	0.940	0.984	0.960	0.969	0.966	0.977	0.965	0.973	0.954	**0.988**	0.981
Geometric mean (GMI)	0.939	0.954	0.976	0.981	0.950	**0.984**	0.973	0.978	0.970	0.983	0.979
Arithmetic mean	0.939	0.954	0.976	0.981	0.951	**0.984**	0.973	0.978	0.970	0.983	0.979

Note: VC1–VC10 represent variable combinations, see table 2 for details; MD represents Mahalanobis distance classifier; numbers in bold represent the highest values for each accuracy category.

Downloaded By: [Li, Zhe] At: 13:52 13 October 2010

Yunnan, China, and ground reference samples were less difficult to collect than the Thai–Lao border site. All 10 output maps from the MLP (figure 2(*b*)) using the 10 different input variable combinations achieved high accuracies and kappa coefficients and appear relatively similar (figure 3). The MLP using the typicalities still outperformed those without using them in terms of GMI (table 4). Best results were achieved from figure 2(*b*): (*n*) and (*r*). The former used VNIR and SWIR together with the typicalities (VC6), and the latter used only typicalities (VC10). For this study site, the MD classifier achieved equivalent or slightly less-accurate results than the MLPs integrating the typicalities. This result suggests that a larger training set leads to less difference between the MLP and the MD classifier and the conventional approach is similarly challenged by limited training samples, as inverting the matrices requires a large sample.

The above results indicate that employing Mahalanobis typicalities as input variables to the MLP is equivalent to introducing ancillary informative feature vectors. This is analogous to incorporating pre-processed or transformed original spectral bands to classifiers to enhance their performance. The well-trained MLP neural network gains information from the typicality maps of each land-cover class and learns to recognize the pattern of 'real' rubber pixels defined by the Mahalanobis typicalities. That is, the MLP was more likely to assign the rubber category to a case that is most typical of the rubber samples encountered in the training set, and thus tends to reduce commission errors for the rubber class.

5. Conclusions

This study conducted rubber classifications using the MLP neural network by integrating Mahalanobis typicalities. Incorporation of Mahalanobis typicalities and MLP neural network facilitates the combination of parametric and non-parametric

models that can take advantage of both approaches. The proposed method can improve MLP's capability of generalization, particularly increasing user's accuracy.

Acknowledgement
This work was funded by NASA Earth System Science grants NNG04GH59G and NX08AL90G. We are grateful to the editor and four anonymous reviewers for their valuable comments and revision on the manuscript.

References

Congalton, R.G., 1991, A review of assessing the accuracy of classifications of remotely sensed data. *Remote Sensing of Environment*, **37**, pp. 35–46.

Eastman, J.R., Toledano, J., Crema, S., Zhu, H. and Jiang, H., 2005, In-process classification assessment of remotely sensed imagery. *GeoCarto International*, **20**, pp. 33–44.

Foody, G.M., 2002, Hard and soft classifications by a neural network with a non-exhaustively defined set of classes. *International Journal of Remote Sensing*, **23**, pp. 3853–3864.

Foody, G.M., Campbell, N.A., Trodd, N.M. and Wood, T.F., 1992, Derivation and applications of probabilistic measures of class membership from the maximum likelihood classification. *Photogrammetric Engineering and Remote Sensing*, **58**, pp. 1335–1341.

Fox, J. and Vogler, J., 2005, Land-use and land-cover change in montane mainland Southeast Asia. *Environmental Management*, **36**, pp. 394–403.

Ghimire, B., Rogan, J. and Miller, J., 2010, Contextual land-cover classification: incorporating spatial dependence in land-cover classification models using random forests and the Getis statistic. *Remote Sensing Letters*, **1**, pp. 45–54.

Hernandez, P.A., Franke, I., Herzog, S.K., Pacheco, V., Paniagua, L., Quintana, H.L., Soto, A., Swenson, J.J., Tovar, C., Valqui, T.H., Vargas, J. and Young, B.E., 2008, Predicting species distributions in poorly-studied landscapes. *Biodiversity Conservation*, **17**, pp. 1353–1366.

Hinton, G.E. and Salakhutdinov, R.R., 2006, Reducing the dimensionality of data with neural networks. *Science*, **313**, pp. 504–507.

Hu, H., Liu, W. and Cao, M., 2008, Impact of land use and land cover changes on ecosystem services in Menglun, Xishuangbanna, Southwest China. *Environmental Monitoring and Assessment*, **46**, pp. 147–156.

Jin, S. and Sader, S.A., 2005, Comparison of time series tasseled cap wetness and the normalized difference moisture index in detecting forest disturbances. *Remote Sensing of the Environment*, **94**, pp. 364–372.

Li, H., Aide, T.M., Ma, Y. and Liu, W., 2007, Demand for rubber is causing the loss of high diversity rain forest in SW China. *Biodiversity Conservation*, **16**, pp. 1731–1745.

Li, Z. and Eastman, J.R., 2010, Commitment and typicality measures for the Self-Organizing Map. *International Journal of Remote Sensing*, **31**, pp. 4265–4280.

Richards, J.A. and Jia, X., 2006, *Remote Sensing Digital Image Analysis: An Introduction, 4th Edition* (Berlin, Heidelberg, Germany: Springer-Verlag).

Roberts, D.A., Numata, I., Holmes, K., Batista, G., Krug, T., Monteiro, A., Powell, B. and Chadwick, O.A., 2002, Large area mapping of land-cover change in Rondonia using multitemporal spectral mixture analysis and decision tree classifiers. *Journal of Geophysical Research*, **107**, p. 8073.

Sangermano, F. and Eastman, J.R., 2007, Linking GIS and ecology – the use of Mahalanobis typicalities to model species distribution. In *Memorias XI Conferencia Iberoamericana de Sistemas de Información Geográfica*, G.D. Buzai (Ed.), pp. 1–13 (Luján: Universidad Nacional de Luján – Sociedad Iberoamericana de Sistemas de Información Geográfica).

Van Ranst, E., Tang, H., Groenemans, R. and Sinthurahat, S., 1996, Application of fuzzy logic to land suitability for rubber production in peninsular Thailand. *Geodema*, **70**, pp. 1–19.

Ziegler, A.D., Fox, J.M. and Xu, J., 2009, The rubber juggernaut. *Science*, **324**, pp. 1024–1025.

Downloaded By: [Li, Zhe] At: 13:52 13 October 2010